Stem Cell Reports
Report
OPEN ACCESS

Induced Pluripotent Stem Cells to Model Human Fibrodysplasia Ossificans Progressiva

Jie Cai,[1] Valeria V. Orlova,[2] Xiujuan Cai,[3] Elisabeth M.W. Eekhoff,[4] Keqin Zhang,[5] Duanqing Pei,[3] Guangjin Pan,[3] Christine L. Mummery,[2] and Peter ten Dijke[1,*]

[1]Department of Molecular Cell Biology, Cancer Genomics Centre Netherlands, Leiden University Medical Center, Leiden 2300, the Netherlands
[2]Department of Anatomy and Embryology, Leiden University Medical Center, Leiden 2300, the Netherlands
[3]Key Laboratory of Regenerative Biology and Guangdong Provincial Key Laboratory of Stem Cell and Regenerative Medicine, South China Institute for Stem Cell Biology and Regenerative Medicine, Guangzhou Institutes of Biomedicine and Health, Chinese Academy of Sciences, Guangzhou 510530, China
[4]Department of Internal Medicine, Endocrine Section, VU University Medical Center, P.O. Box 7057, Amsterdam 1007, the Netherlands
[5]Department of Endocrinology, Tongji Hospital Affiliated with Tongji University, Shanghai 200065, China
*Correspondence: p.ten_dijke@lumc.nl
http://dx.doi.org/10.1016/j.stemcr.2015.10.020

SUMMARY

Fibrodysplasia ossificans progressiva (FOP) is a rare disease characterized by progressive ossification of soft tissues, for which there is no effective treatment. Mutations in the bone morphogenetic protein (BMP) type I receptor activin receptor-like kinase 2 (ACVR1/ALK2) are the main cause of FOP. We generated human induced pluripotent stem cells (hiPSCs) from FOP patients with the ALK2 R206H mutation. The mutant *ALK2* gene changed differentiation efficiencies of hiPSCs into FOP bone-forming progenitors: endothelial cells (ECs) and pericytes. ECs from FOP hiPSCs showed reduced expression of vascular endothelial growth factor receptor 2 and could transform into mesenchymal cells through endothelial-mesenchymal transition. Increased mineralization of pericytes from FOP hiPSCs could be partly inhibited by the ALK2 kinase inhibitor LDN-212854. Thus, differentiated FOP hiPSCs recapitulate some aspects of the disease phenotype in vitro, and they could be instrumental in further elucidating underlying mechanisms of FOP and development of therapeutic drug candidates.

INTRODUCTION

Fibrodysplasia ossificans progressiva (FOP) is an autosomal dominant genetic disorder in which acute inflammation may trigger the formation of a second skeleton of heterotopic bone. Classic FOP is caused by gain-of-function mutation (617G > A; R206H) in the activin receptor-like kinase 2 (ACVR1/ALK2) gene, encoding the bone morphogenetic protein (BMP) type I receptor (Shore et al., 2006). Enhanced BMP signaling in patients with the ALK2 R206H mutation has been attributed to loss of inhibitory activity of the ALK2-interacting protein FK506-binding protein-12 (FKBP12) (Chaikuad et al., 2012; van Dinther et al., 2010). Previous publications indicated that Tie2$^+$ endothelial cells (ECs) and mesenchymal cells (MCs) contributed as progenitor cells to the episodic heterotopic ossification (HO) in FOP (Medici et al., 2010; Wosczyna et al., 2012). Other cells like circulating osteogenic precursors, skeletal myoblasts, and vascular smooth muscle cells also were found in FOP lesions and may contribute to HO in FOP (Hegyi et al., 2003; Lounev et al., 2009; Suda et al., 2009).

Despite recent advances in understanding of the disease (Hatsell et al., 2015), to date there is no cure or even treatment for HO in FOP. A comprehensive understanding of the molecular mechanisms underlying abnormal behavior of bone-forming progenitor cells in FOP could be one approach toward effective treatment for HO in FOP, and to other more prevalent situations with HO that, for example, may occur after traumatic accidents or deep tissue burns. The traditional way of obtaining human biopsy tissues from FOP patients is limited as physical and surgical injury can induce HO. New protocols to produce well-characterized FOP bone-forming progenitor cells for research and therapeutic drug screening are needed. The ability to generate human induced pluripotent stem cells (hiPSCs) (Takahashi et al., 2007) from adult tissues provides new opportunities for research on FOP. If derived from patients with genetic disease, hiPSCs allow production of large numbers of diseased target cells for basic research and drug development since they are immortal and pluripotent (Sterneckert et al., 2014).

In this study, we generated FOP hiPSCs from kidney cells isolated from urine by episomal vectors. The expression of pluripotent markers and ability to form derivatives of the three germ layers were comparable in FOP and control hiPSCs. However, the mutation in ALK2 reduced the efficiency of differentiation of hiPSCs into ECs and affected the phenotypes of ECs and pericytes. The hiPSC-derived ECs (hiPSC-ECs) from FOP patients exhibited reduced expression of vascular endothelial growth factor receptor 2 (VEGFR2) and could be transformed into MCs through endothelial-mesenchymal transition (EndMT). The hiPSC-derived pericytes (hiPSC-pericytes) from the FOP group showed increased ability to mineralize compared with the

control. Our experiments demonstrated that disease-relevant cells differentiated from FOP hiPSCs possessed phenotypes reminiscent of the FOP disease.

RESULTS

Generation of FOP hiPSCs from Urine Cells

We used a rapid and non-invasive procedure to isolate kidney cells in urine from FOP patients (Xue et al., 2013). The cells were isolated from 50–100 ml middle stream of the micturition from two male FOP patients (Dutch and Chinese, F2 and F3) diagnosed with the classic R206H mutation and two healthy male donors (Dutch and Chinese, C2 and C3) (Figure S1B).

A schematic representation of hiPSC generation is shown in Figure S1A. In summary, cultured cells from urine were electroporated with episomal vectors containing *OCT4*, *SOX2*, *KLF4*, and the *pCEP4-miR-302-367* cluster (containing *miR-302b*, *c*, *a*, *d*, and *miR-367*) (Xue et al., 2013). Transfected urine cells were maintained in serum-free mTesR1 medium supplemented with a cocktail of small molecule inhibitors to promote reprogramming: CHIR99021, PD0325901, A83-01, and thiazovivin (Wang et al., 2013). Small colonies of cells appeared that progressively adopted a human embryonic stem cell (hESC)-like morphology. Selected hiPSCs were picked manually and expanded at day 20; hiPSCs maintained their hESC-like morphology with prominent nuclei and little cytoplasm and stained positive for alkaline phosphatase (ALP) (Figure S1B).

The hiPSCs from one healthy donor (C3) and from two FOP patients (F2 and F3) were characterized; the other control hiPSC line (UE017C1) was obtained from the Guangzhou Stem Cell Bank produced by the same method and was characterized previously (Xue et al., 2013). The presence of classical mutation in the *ALK2* gene was confirmed in FOP hiPSCs (Figure S1C). FOP and control hiPSC karyotypes were checked before passage 10 and these were normal (Figure S1D). The loss of exogenous reprogramming factors and episomal backbones was demonstrated by genomic PCR that specifically amplifies exogenous factors (Figure S1E). The quantitative real-time PCR analysis revealed that, compared to urine cells, FOP hiPSCs had upregulated expression of endogenous hESC transcriptional genes (endogenous *OCT4*, endogenous *SOX2*, *NANOG*, and *REX1*), and they had expression levels comparable with established H1 hESCs (Figure S1F). Immunofluorescence microscopy showed expression of pluripotency-associated antigens OCT4, SSEA-4, TRA-1-60, and TRA-1-81 (Figure S1G). In addition, hiPSCs formed teratomas in mice in vivo, confirming the pluripotency of FOP iPSCs (Figure S1H). Therefore, hiPSCs from FOP patients corresponded phenotypically and functionally to hESCs.

Impaired EC Differentiation of FOP hiPSCs

A slight elevation of pSMAD1/5 signaling in FOP hiPSCs compared to control hiPSCs was observed when these cells were cultured for 24 hr in medium with low serum concentrations, but not in the undifferentiated FOP iPSCs (Figures 1A and S1I). We differentiated hiPSCs into ECs and pericytes to examine how minor changes in ALK2 R206H/SMAD signaling influenced the fate of two possible progenitor cells of FOP, i.e., ECs and pericytes. On days 10–12 of differentiation, flow cytometry (fluorescence-activated cell sorting [FACS]) analysis showed that two cell populations formed as follows: $CD31^+$ ECs and platelet-derived growth factor receptor (PDGFR) β^+ pericytes (Figure 1B). The generation of $CD31^+$/VE-$cadherin^+$ cells was significantly impaired in FOP hiPSCs compared with controls, while general mesoderm induction was slightly enhanced in FOP hiPSCs (Figures 1B and 1C).

To verify the FACS data, we examined the expression of early mesoderm and EC-specific genes (Figure 1D). Differentiation resulted in efficient downregulation of pluripotent markers (*OCT4* and *NANOG*) in the control and FOP hiPSCs. Primitive streak/mesoderm lineage markers (*T* and *PDGFRα*) were upregulated in FOP hiPSCs on day 4 of differentiation, which may due to the positive effect of the BMP-signaling pathway on mesoderm formation. The induction of the early endothelial transcription factor (*ETV2*) on day 4 was similar between the two groups. However, consistent with the FACS data, we observed that endothelial-specific genes (*CD31* and *CD105*) were downregulated in FOP hiPSCs on day 7 of differentiation. Early pericyte markers *PDGFRβ* and *NG2* proteoglycan were expressed more abundantly in differentiating FOP hiPSCs. Overall, we observed that the EC differentiation efficiency was impaired while general mesoderm differentiation was enhanced in FOP hiPSCs; this difference may due to the elevated level of ALK2 R206H/SMAD signaling in FOP compared to control hiPSCs.

Characterization of FOP hiPSC-ECs

Differentiated cell populations were divided into $CD31^+$ ECs and $CD31^-$ cells by CD31 antibody-coupled magnetic bead sorting (Figure 2A). The expression levels of BMP type I receptors ALK1 and ALK2 were not different in control versus FOP $CD31^+$ cells (Figure S2A). Sorted FOP hiPSC-ECs were more sensitive to low concentrations of BMP6 (5 ng/ml) and the activated BMP signaling could be inhibited by BMP type I receptor kinase inhibitor LDN-193189 (Yu et al., 2008; Figure 2B). FOP hiPSC-ECs exhibited poor viability and increased expression of senescence-associated β-galactosidase expression compared to controls (Figures S2B and S2C). As the VEGF-signaling pathway is known to regulate survival and proliferation of ECs through VEGFR2 (Kelly and Hirschi, 2009), we

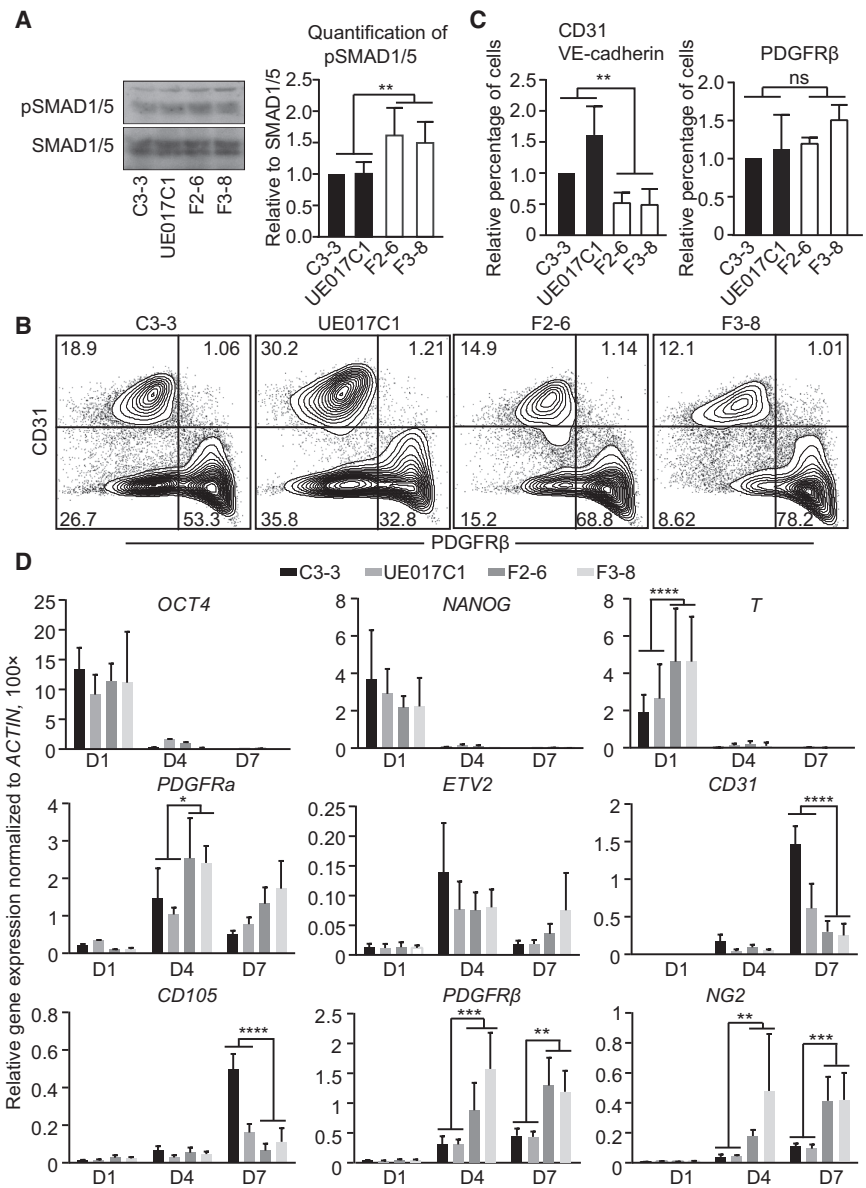

Figure 1. Differentiation of FOP hiPSCs into ECs and Pericytes

(A) Total SMAD1/5 and phospho-SMAD1/5 (pSMAD1/5) level in control hiPSCs (C3-3 and UE017C1) and FOP hiPSCs (F2-6 and F3-8). Note that the antibodies used here also may recognize SMAD8 and pSMAD8 bands.

(B) FACS analysis of EC marker (CD31) or pericyte marker (PDGFRβ) expression at differentiation days 10–12 is shown.

(C) Quantification of the FACS analysis data for relative percentage of CD31 and VE-cadherin double-positive ECs and PDGFRβ-positive pericytes. All values were adjusted to the control colony C3-3, which is defined as 1.

(D) Relative gene expression at different time points during the differentiation. *ACTIN* was used to normalize gene expression.

Data are presented as mean and SD from three independent experiments in (A), (C), and (D).

found that the expression of VEGFR2 was lower in FOP hiPSC-ECs compared with the control by FACS analysis, while the expression levels of other EC genes (CD31 and VE-cadherin) were unchanged (Figure 2C). The lower expression of VEGFR2 may be responsible for the failure of FOP hiPSC-ECs to propagate in vitro, and this may be related to the activated BMP/SMAD signaling in these cells (Figure 2B).

Moreover, we observed that ECs cultured in EGM-2 medium with 2% serum showed increased expression of EndMT markers (*SLUG*, *N-cadherin*, and *TWIST*; Figure 2D) and lost the expression of endothelial-specific markers confirmed by quantitative real-time PCR (*VE-cadherin* and *VEGFR2*; Figure 2D) and FACS analysis (CD31, VE-cadherin, and VEGFR2; Figure S2D). ECs turned to mesenchymal-like cells (EC-MCs) in EGM2 medium and the expression of mesenchymal markers CD73, CD90, and CD105 also were induced (Figures 2E, 2F, and S2E). BMP signaling also was activated at an elevated level in FOP EC-MCs, as demonstrated by increased *ID1* expression (Figure 2G), a direct BMP/SMAD target gene (Korchynskyi and ten Dijke, 2002). Therefore, increased BMP signaling in FOP hiPSC-ECs correlates with impaired EC viability, increased senescence, and increased EndMT.

Activated BMP Signaling in FOP hiPSC-Pericytes

The selected CD31$^-$ cells were cultured in DMEM with 10% fetal bovine serum (FBS) or DMEM with 10% FBS

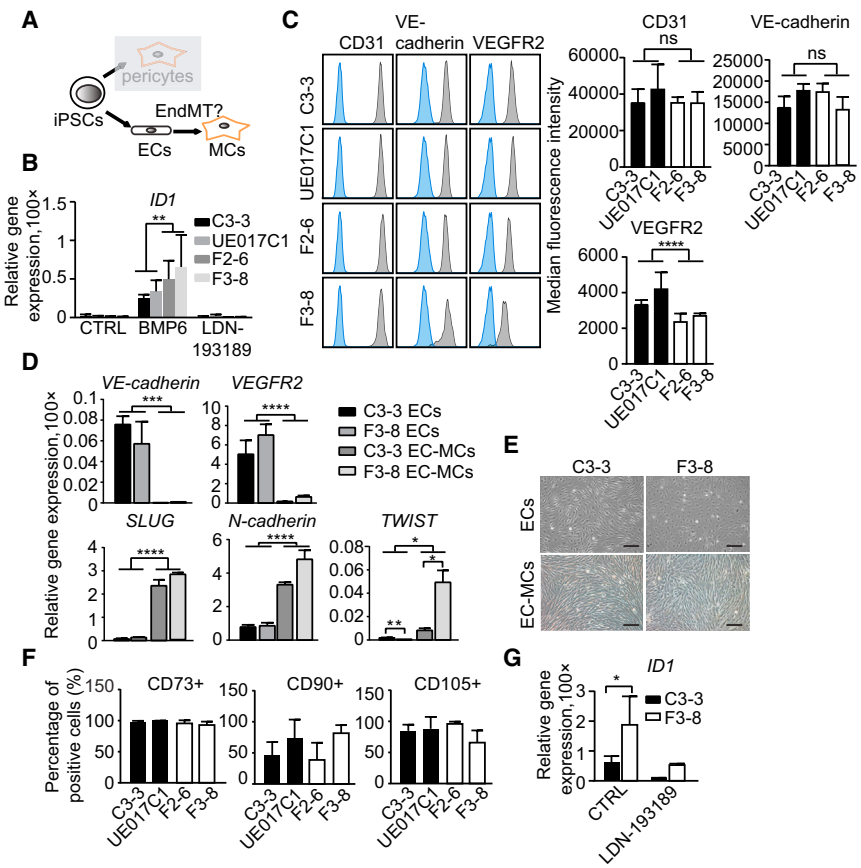

Figure 2. ECs Derived from hiPSCs Undergo EndMT

(A) Schematic representation shows EC and pericyte derivation from hiPSCs.

(B) Analysis of relative expression of *ID1* in hiPSC-ECs is shown.

(C) (Left) Representative FACS analysis for EC markers in hiPSC-ECs is shown. Blue, unstained cells; gray, antibody as indicated. (Right) Median fluorescence intensity of EC markers expression in hiPSC-ECs is shown.

(D) Relative gene expression analysis of EC and EndMT markers in ECs and EC-MCs is shown.

(E) Bright-field images of ECs and EC-MCs in the healthy donor (C3-3) and FOP patient (F3-8) are shown. Scale bar, 100 μm.

(F) Percentages of CD73-, CD90-, and CD105-positive cells in EC-MCs. Representative FACS plots of CD73, CD90, and CD105 are shown in Figure S2E.

(G) Relative expression of *ID1* in EC-MCs is shown.

Data are presented as mean and SD from three independent experiments in (B), (C), (D), (F), and (G). The quantitative real-time PCR results in (B), (D), and (G) were normalized to *ACTIN*. See also Figure S2.

supplemented with PDGF-BB and transforming growth factor (TGF) β3 for 1 day. The homogenous population expressed pericytes and MC markers (CD73, CD90, CD105, PDGFRβ, CD146, and NG2; Figures 3A, 3B, and S3A). SMAD1/5 phosphorylation was increased in the FOP group in low-serum conditions, and this could be inhibited by LDN-193189 (Figure 3C). The mRNA expression level of *ALK2* was not different in control and FOP groups (Figure S3B). The SMAD1/5 downstream target gene *ID1* also was significantly upregulated in the FOP group (Figure 3D). Thus, FOP hiPSC-pericytes exhibited elevated SMAD1/5 levels.

FOP hiPSC-Pericyte Mineralization as an Assay to Identify New ALK2 Inhibitors

Heterotopic bone formation in FOP follows the progressive heterotopic endochondral ossification in soft connective tissues, a process in which condensing mesenchymal progenitor cells differentiate into chondrocytes and are eventually mineralized into osteoblasts and bone (Mackie et al., 2011). We examined the effect of ALK2 R206H mutation on chondrogenic differentiation by differentiating hiPSC-pericytes in the two-dimensional micromass culture system without the addition of growth factors. The hiPSC-pericytes were stained with Alcian blue for early differentiation and extracellular matrix production, such as glycosaminoglycans (GAGs) and sulfated GAGs. After 3 days of chondrocytic differentiation, Alcian blue staining indicated that FOP hiPSC-pericytes have more GAG expression than control hiPSC-pericytes (Figures 4A and 4B).

We further assessed the mineralization capability of FOP hiPSC-pericytes when grown in osteogenic medium. The osteoblast differentiation of pericytes was measured by determining ALP activity, an early marker of osteoblast differentiation. Histochemical staining revealed that ALP activity in the FOP group was enhanced (Figure 4C); F2-6 hiPSC-pericytes showed higher pSMAD1/5 signaling compared to F3-8 (Figures 3C and 3D), which may explain the stronger ALP activity in F2-6. Furthermore, we analyzed osteoblast differentiation by alizarin red S staining to detect calcium deposition. On day 21 and day 28 of differentiation, we detected higher mineralization in the FOP group (Figures 4D and 4E). Consistent with the ALP activity and alizarin red S staining, quantitative real-time PCR analysis confirmed that expression of osteoblast markers *ALP* and *OSTEOCALCIN* (*OSC*) (Figure 4F) was increased in the

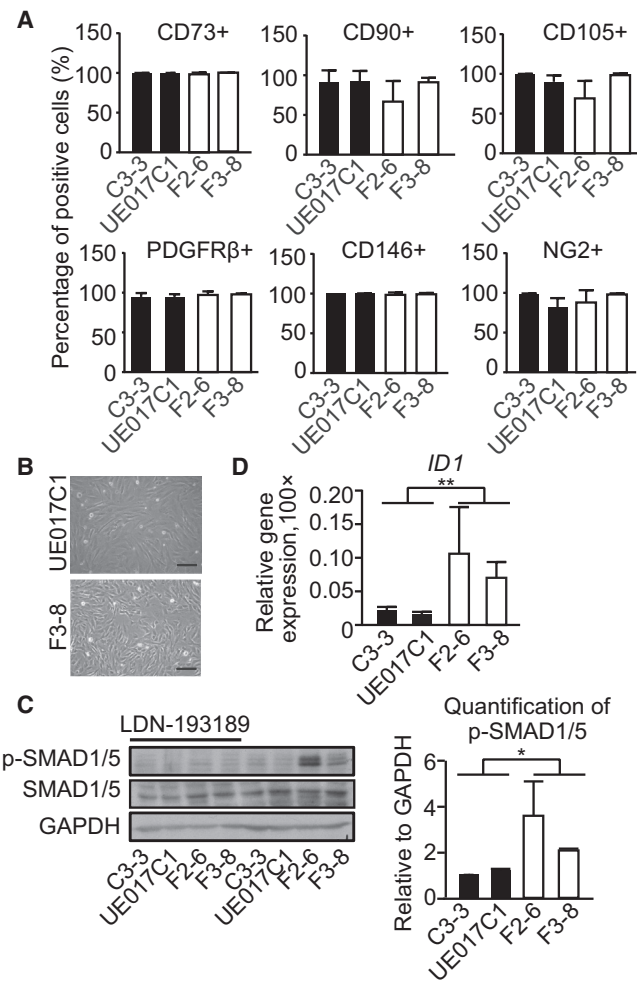

Figure 3. Activated BMP Signaling in FOP hiPSC-Pericytes

(A) Percentages of CD73-, CD90-, CD105-, PDGFRβ-, CD146-, and NG2-positive cells in hiPSC-pericytes. Representative FACS plots of CD73, CD90, CD105, PDGFRβ, CD146, and NG2 are shown in Figure S3A.

(B) Bright-field images of pericytes from healthy donor (UE017C1) and FOP patient (F3-8) are shown. Scale bar, 100 μm.

(C) Western blot results showing SMAD1/5 phosphorylation in the hiPSC-pericytes. GAPDH was used as the loading control.

(D) Relative expression of *ID1*. All experiments were normalized to *ACTIN*.

Data are presented as mean and SD from three independent experiments in (C) and (D); the average of four independent experiments is shown in (A). See also Figure S3.

FOP group, but we did not detect altered expression of *COLLAGEN type I alpha 1 (COL1α)* in FOP and control cells (Figure 4F). Together these data indicate that FOP hiPSC-pericytes were prone to mineralization, which may be due to activated BMP/SMAD signal in these cells. After pretreating pericytes with LDN-212854, a BMP type I receptor kinase inhibitor that is more selective for ALK2 compared with other BMP type I receptors (Mohedas et al., 2013), we observed that the ALP activity of FOP hiPSC-pericytes was partly inhibited (Figure 4G).

DISCUSSION

Our results demonstrated that hiPSCs could be used as an in vitro disease model for FOP. The hiPSC-ECs and hiPSC-pericytes can be applied to investigate the molecular mechanisms underlying the pathology of FOP, as well as to identify new therapeutic drugs.

We have shown that FOP hiPSCs could be established from cells in urine using non-integrating episomal vectors. BMP signaling contributes to the initial stage of iPSC reprogramming in mouse (Samavarchi-Tehrani et al., 2010), but induces differentiation of hESCs (Xu et al., 2002). Consistent with prior research (Matsumoto et al., 2013), our FOP hiPSCs were generated without the addition of exogenous BMP inhibitors during the reprogramming process. We did not observe activated SMAD1/5 signaling in FOP hiPSCs maintained in hESC medium mTeSR1 unless these cells were placed in differentiation culture conditions. This may explain why FOP hiPSCs could be maintained and passaged in defined medium. Besides, we observed heterogeneous BMP/SMAD signaling and mineralization in FOP hiPSCs and derivative cells, indicating that intrinsic genetic and/or epigenetic features of donor cells may influence properties of hiPSCs and the progeny. To eliminate the heterogeneity, the isogenic correction FOP hiPSCs can help to facilitate more stringent screening for effects arising from clonal variations in hiPSCs (Matsumoto et al., 2015).

We found that the generation and maintenance of ECs from FOP hiPSCs were impaired. One explanation is the elevated BMP signaling in FOP hiPSC-ECs, which resulted in downregulation of VEGFR2 expression that mediated VEGF-induced proliferation and survival of ECs; this may have caused the decrease in EC viability. Inhibition of BMP receptor kinase activity by LDN-212854 during the vascular specification stage (from day 3 of hiPSC differentiation) did not rescue the impaired FOP hiPSC-EC phenotypes (unpublished data). BMPs are indispensable for the formation of mesoderm where ECs originate, but they may function as a context-dependent regulator in vascular morphogenesis (Kim et al., 2014). In addition, a recent publication indicated activin A signals through the mutant ALK2 R206H to stimulate HO in FOP conditional-on knockin mice (Hatsell et al., 2015). Of note, in our EC differentiation protocol, we used activin A and BMP4, both of which were shown to induce SMAD1/5 signaling through mutant ALK2 R206H (Hatsell et al., 2015). These ligands may thus combine with the SMAD1/5 signal to

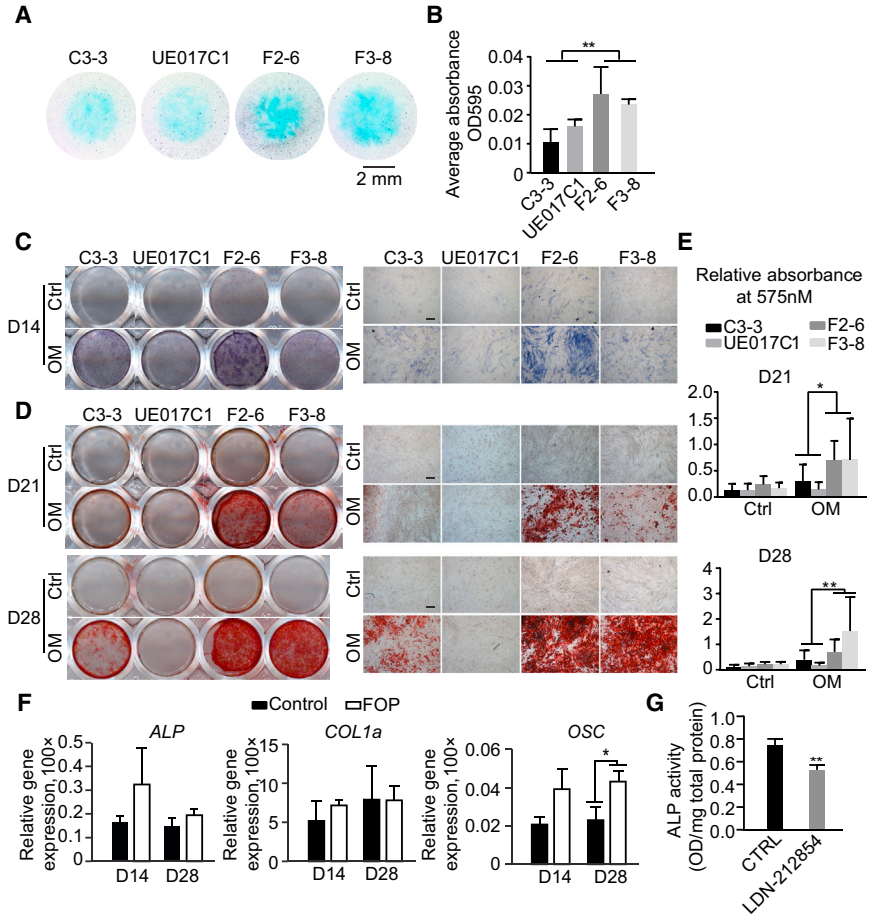

Figure 4. Increased Mineralization of FOP hiPSC-Pericytes

(A) Representative Alcian blue staining of the micromass for 3 days chondrogenic differentiation is shown. Scale bar, 2 mm.

(B) Alcian blue staining of micromasses was quantified by stain extraction and absorbance reading at 595 nm.

(C) ALP staining was performed 14 days (D14) after maintaining in α-MEM with 10% FBS (Ctrl) and osteogenic medium (OM). Results are shown as representative scanned images (left) and images taken at 4× magnification (right). Scale bar, 200 μm.

(D) The mineralization was visualized by 2% alizarin red S staining on day 21 (D21) and day 28 (D28). Results are shown as representative scanned images (left) and images taken at 4× magnification (right). Scale bar, 200 μm.

(E) Alizarin red S staining on D21 and D28 was quantified by stain extraction and absorbance reading at 570 nm.

(F) Relative gene expression analysis of *ALP*, *COL1α*, and *OSC* on day 14 and day 28 of osteoblast differentiation. All experiments were normalized to *ACTIN*. Control, the average of the results from C3-3 and UE017C1; FOP, the average of the results from F2-6 and F3-8.

(G) ALP assay on day 7 of F3-8 after maintaining in OM pretreated with LDN-212854 is shown.

Data are presented as mean and SD from four times independent experiments in (E) and three times in (B) and (G).

contribute to the FOP hiPSC-EC phenotypes that we observed. The other explanation of low EC yields is the increased EndoMT in ALK2-mutated ECs. Consistent with a previous publication (Medici et al., 2010), FOP EC-MCs showed higher expression of EndMT markers (*N-cadherin* and *TWIST*), which might be due to the interaction of mutant ALK2 R206H and VEGF signaling in these cells. Further investigation of the crosstalk between BMP signaling and VEGF signaling might contribute to the better understanding of the EndMT mechanism in FOP lesions and also help in identifying new drug-treatable targets to prevent HO in FOP patients.

Lastly, we demonstrated that the mutant ALK2 R206H contributed to the increased mineralization of FOP hiPSC-pericytes and, as such, is a useful human in vitro disease model for identifying and evaluating the bioactivity of ALK2 inhibitors. More evidence indicates that MCs are the major contributors of HO (Wosczyna et al., 2012), while ECs indirectly contribute to osteogenic differentiation by acting in a paracrine manner via crosstalk between ECs and MCs (Bidarra et al., 2011; Lin et al., 2014). Even though Matsumoto et al. partly exhibited FOP phenotypes by directly differentiating hiPSCs into osteoblast cells (Matsumoto et al., 2013), they provided little evidence of how the specific cell types contributed to the increased mineralization. To further clarify the mineralization capacity of FOP hiPSCs in vitro, we differentiated hiPSCs into pericytes. ALP activity of FOP hiPSC-pericytes can be inhibited by pretreating with BMP inhibitor LDN-212854. As the ALP assay has been used as a high-throughput screening (HTS) readout for screening regulators in osteogenic differentiation (Alves et al., 2011), our platform could be used for drug screening and further verifying the bioactivity of ALK2 inhibitors in the future.

Even though in this study we only studied ECs and pericytes, the two most well-known HO progenitor cells in FOP, it is possible other unidentified cells types also may be involved in the HO process in FOP. Due to the pluripotent

characterization of hiPSCs, FOP hiPSCs can be differentiated into other (unknown) progenitor cells to discover the underlying molecular mechanisms of HO in the future.

EXPERIMENTAL PROCEDURES

Primary human cells were obtained with informed consent. Experiments involving human subjects were approved by Institutional Review Board (IRB) GIBH-IRB02-2009002 at Guangzhou Institutes of Biomedicine and Health (GIBH) and 12/467 (2013 January) at VU University Medical Center. The animal research was approved by the IRB at GIBH (2010012). The generation and differentiation of hiPSCs were described previously (Orlova et al., 2014; Xue et al., 2013). Differences between the control group and the FOP group were evaluated by t test or one-way ANOVA with Tukey's multiple comparison tests (ns, not significant; *$p < 0.05$, **$p < 0.01$, ***$p < 0.001$, and ****$p < 0.0001$). For further information, see the Supplemental Experimental Procedures.

SUPPLEMENTAL INFORMATION

Supplemental Information includes Supplemental Experimental Procedures and three figures and can be found with this article online at http://dx.doi.org/10.1016/j.stemcr.2015.10.020.

AUTHOR CONTRIBUTIONS

J.C., V.V.O., X.C., G.P., and P.t.D. planned the experiments. E.M.W.E. and K.Z. provided patients materials. J.C. and V.V.O. performed research and acquired data. J.C. analyzed data and wrote the paper. D.P., C.L.M., G.P., and P.t.D. supervised the project.

ACKNOWLEDGMENTS

We would like to acknowledge Keyu Lai for performing karyotype of hiPSCs, Jian Zhang for performing teratoma injection, Dr. Ke Ding and Dr. Paul Yu for providing reagents, Dr. Amaya García de Vinuesa for helpful suggestions on chondrogenic differentiation, Dr. Gerard Pals for help with urine collection from Dutch patients, and Francijna E.van den Hil for help with the preparation of EC differentiation and EC sorting. This work was supported by the LeDucq Foundation, the China Exchange Programme (CEP) of the Royal Netherlands Academy of Arts and Sciences (KNAW), and the European Community's Seventh Framework Programme (FP7/2007-2013) under grant agreement 602423: Plurimes.

Received: April 27, 2015
Revised: October 29, 2015
Accepted: October 29, 2015
Published: November 25, 2015

REFERENCES

Alves, H., Dechering, K., Van Blitterswijk, C., and De Boer, J. (2011). High-throughput assay for the identification of compounds regulating osteogenic differentiation of human mesenchymal stromal cells. PLoS ONE *6*, e26678.

Bidarra, S.J., Barrias, C.C., Barbosa, M.A., Soares, R., Amédée, J., and Granja, P.L. (2011). Phenotypic and proliferative modulation of human mesenchymal stem cells via crosstalk with endothelial cells. Stem Cell Res. *7*, 186–197.

Chaikuad, A., Alfano, I., Kerr, G., Sanvitale, C.E., Boergermann, J.H., Triffitt, J.T., von Delft, F., Knapp, S., Knaus, P., and Bullock, A.N. (2012). Structure of the bone morphogenetic protein receptor ALK2 and implications for fibrodysplasia ossificans progressiva. J. Biol. Chem. *287*, 36990–36998.

Hatsell, S.J., Idone, V., Wolken, D.M., Huang, L., Kim, H.J., Wang, L., Wen, X., Nannuru, K.C., Jimenez, J., Xie, L., et al. (2015). ACVR1R206H receptor mutation causes fibrodysplasia ossificans progressiva by imparting responsiveness to activin A. Sci. Transl. Med. *7*, 303ra137.

Hegyi, L., Gannon, F.H., Glaser, D.L., Shore, E.M., Kaplan, F.S., and Shanahan, C.M. (2003). Stromal cells of fibrodysplasia ossificans progressiva lesions express smooth muscle lineage markers and the osteogenic transcription factor Runx2/Cbfa-1: clues to a vascular origin of heterotopic ossification? J. Pathol. *201*, 141–148.

Kelly, M.A., and Hirschi, K.K. (2009). Signaling hierarchy regulating human endothelial cell development. Arterioscler. Thromb. Vasc. Biol. *29*, 718–724.

Kim, J.D., Lee, H.W., and Jin, S.W. (2014). Diversity is in my veins: role of bone morphogenetic protein signaling during venous morphogenesis in zebrafish illustrates the heterogeneity within endothelial cells. Arterioscler. Thromb. Vasc. Biol. *34*, 1838–1845.

Korchynskyi, O., and ten Dijke, P. (2002). Identification and functional characterization of distinct critically important bone morphogenetic protein-specific response elements in the Id1 promoter. J. Biol. Chem. *277*, 4883–4891.

Lin, R.Z., Moreno-Luna, R., Li, D., Jaminet, S.C., Greene, A.K., and Melero-Martin, J.M. (2014). Human endothelial colony-forming cells serve as trophic mediators for mesenchymal stem cell engraftment via paracrine signaling. Proc. Natl. Acad. Sci. USA *111*, 10137–10142.

Lounev, V.Y., Ramachandran, R., Wosczyna, M.N., Yamamoto, M., Maidment, A.D., Shore, E.M., Glaser, D.L., Goldhamer, D.J., and Kaplan, F.S. (2009). Identification of progenitor cells that contribute to heterotopic skeletogenesis. J. Bone Joint Surg. Am. *91*, 652–663.

Mackie, E.J., Tatarczuch, L., and Mirams, M. (2011). The skeleton: a multi-functional complex organ: the growth plate chondrocyte and endochondral ossification. J. Endocrinol. *211*, 109–121.

Matsumoto, Y., Hayashi, Y., Schlieve, C.R., Ikeya, M., Kim, H., Nguyen, T.D., Sami, S., Baba, S., Barruet, E., Nasu, A., et al. (2013). Induced pluripotent stem cells from patients with human fibrodysplasia ossificans progressiva show increased mineralization and cartilage formation. Orphanet J. Rare Dis. *8*, 190.

Matsumoto, Y., Ikeya, M., Hino, K., Horigome, K., Fukuta, M., Watanabe, M., Nagata, S., Yamamoto, T., Otsuka, T., and Toguchida, J. (2015). New Protocol to Optimize iPS Cells for Genome Analysis of Fibrodysplasia Ossificans Progressiva. Stem Cells *33*, 1730–1742.

Medici, D., Shore, E.M., Lounev, V.Y., Kaplan, F.S., Kalluri, R., and Olsen, B.R. (2010). Conversion of vascular endothelial cells into multipotent stem-like cells. Nat. Med. *16*, 1400–1406.

Mohedas, A.H., Xing, X., Armstrong, K.A., Bullock, A.N., Cuny, G.D., and Yu, P.B. (2013). Development of an ALK2-biased BMP type I receptor kinase inhibitor. ACS Chem. Biol. *8*, 1291–1302.

Orlova, V.V., Drabsch, Y., Freund, C., Petrus-Reurer, S., van den Hil, F.E., Muenthaisong, S., Dijke, P.T., and Mummery, C.L. (2014). Functionality of endothelial cells and pericytes from human pluripotent stem cells demonstrated in cultured vascular plexus and zebrafish xenografts. Arterioscler. Thromb. Vasc. Biol. *34*, 177–186.

Samavarchi-Tehrani, P., Golipour, A., David, L., Sung, H.K., Beyer, T.A., Datti, A., Woltjen, K., Nagy, A., and Wrana, J.L. (2010). Functional genomics reveals a BMP-driven mesenchymal-to-epithelial transition in the initiation of somatic cell reprogramming. Cell Stem Cell *7*, 64–77.

Shore, E.M., Xu, M., Feldman, G.J., Fenstermacher, D.A., Cho, T.J., Choi, I.H., Connor, J.M., Delai, P., Glaser, D.L., LeMerrer, M., et al. (2006). A recurrent mutation in the BMP type I receptor ACVR1 causes inherited and sporadic fibrodysplasia ossificans progressiva. Nat. Genet. *38*, 525–527.

Sterneckert, J.L., Reinhardt, P., and Schöler, H.R. (2014). Investigating human disease using stem cell models. Nat. Rev. Genet. *15*, 625–639.

Suda, R.K., Billings, P.C., Egan, K.P., Kim, J.H., McCarrick-Walmsley, R., Glaser, D.L., Porter, D.L., Shore, E.M., and Pignolo, R.J. (2009). Circulating osteogenic precursor cells in heterotopic bone formation. Stem Cells *27*, 2209–2219.

Takahashi, K., Tanabe, K., Ohnuki, M., Narita, M., Ichisaka, T., Tomoda, K., and Yamanaka, S. (2007). Induction of pluripotent stem cells from adult human fibroblasts by defined factors. Cell *131*, 861–872.

van Dinther, M., Visser, N., de Gorter, D.J., Doorn, J., Goumans, M.J., de Boer, J., and ten Dijke, P. (2010). ALK2 R206H mutation linked to fibrodysplasia ossificans progressiva confers constitutive activity to the BMP type I receptor and sensitizes mesenchymal cells to BMP-induced osteoblast differentiation and bone formation. J. Bone Miner. Res. *25*, 1208–1215.

Wang, L., Wang, L., Huang, W., Su, H., Xue, Y., Su, Z., Liao, B., Wang, H., Bao, X., Qin, D., et al. (2013). Generation of integration-free neural progenitor cells from cells in human urine. Nat. Methods *10*, 84–89.

Wosczyna, M.N., Biswas, A.A., Cogswell, C.A., and Goldhamer, D.J. (2012). Multipotent progenitors resident in the skeletal muscle interstitium exhibit robust BMP-dependent osteogenic activity and mediate heterotopic ossification. J. Bone Miner. Res. *27*, 1004–1017.

Xu, R.H., Chen, X., Li, D.S., Li, R., Addicks, G.C., Glennon, C., Zwaka, T.P., and Thomson, J.A. (2002). BMP4 initiates human embryonic stem cell differentiation to trophoblast. Nat. Biotechnol. *20*, 1261–1264.

Xue, Y., Cai, X., Wang, L., Liao, B., Zhang, H., Shan, Y., Chen, Q., Zhou, T., Li, X., Hou, J., et al. (2013). Generating a non-integrating human induced pluripotent stem cell bank from urine-derived cells. PLoS ONE *8*, e70573.

Yu, P.B., Deng, D.Y., Lai, C.S., Hong, C.C., Cuny, G.D., Bouxsein, M.L., Hong, D.W., McManus, P.M., Katagiri, T., Sachidanandan, C., et al. (2008). BMP type I receptor inhibition reduces heterotopic [corrected] ossification. Nat. Med. *14*, 1363–1369.

Stem Cell Reports, Volume *5*

Supplemental Information

Induced Pluripotent Stem Cells to Model Human Fibrodysplasia Ossificans Progressiva

Jie Cai, Valeria V. Orlova, Xiujuan Cai, Elisabeth M.W. Eekhoff, Keqin Zhang, Duanqing Pei, Guangjin Pan, Christine L. Mummery, and Peter ten Dijke

Figure S1

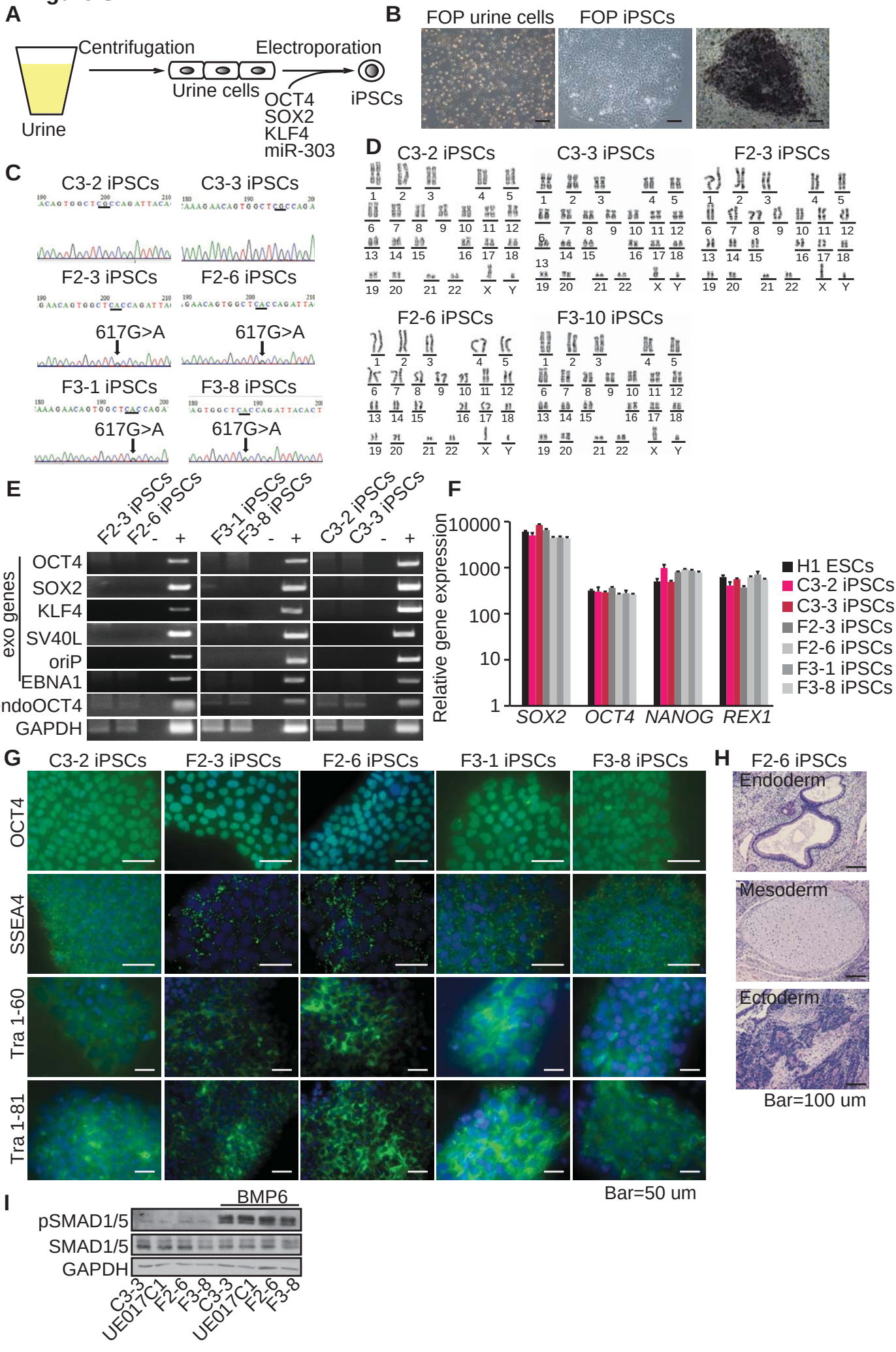
A
Centrifugation
Electroporation
Urine cells
Urine
OCT4
SOX2
KLF4
miR-303
iPSCs
B
FOP urine cells
FOP iPSCs
C
C3-2 iPSCs
C3-3 iPSCs
F2-3 iPSCs
F2-6 iPSCs
617G>A
617G>A
F3-1 iPSCs
F3-8 iPSCs
617G>A
617G>A
D
C3-2 iPSCs
C3-3 iPSCs
F2-3 iPSCs
F2-6 iPSCs
F3-10 iPSCs
E
F2-3 iPSCs
F2-6 iPSCs
F3-1 iPSCs
F3-8 iPSCs
C3-2 iPSCs
C3-3 iPSCs
- +
exo genes
OCT4
SOX2
KLF4
SV40L
oriP
EBNA1
endoOCT4
GAPDH
F
Relative gene expression
10000
1000
100
10
1
SOX2
OCT4
NANOG
REX1
H1 ESCs
C3-2 iPSCs
C3-3 iPSCs
F2-3 iPSCs
F2-6 iPSCs
F3-1 iPSCs
F3-8 iPSCs
G
C3-2 iPSCs
F2-3 iPSCs
F2-6 iPSCs
F3-1 iPSCs
F3-8 iPSCs
OCT4
SSEA4
Tra 1-60
Tra 1-81
Bar=50 um
H
F2-6 iPSCs
Endoderm
Mesoderm
Ectoderm
Bar=100 um
I
BMP6
pSMAD1/5
SMAD1/5
GAPDH
C3-3
UE017C1
F2-6
F3-8
C3-3
UE017C1
F2-6
F3-8

Figure S2

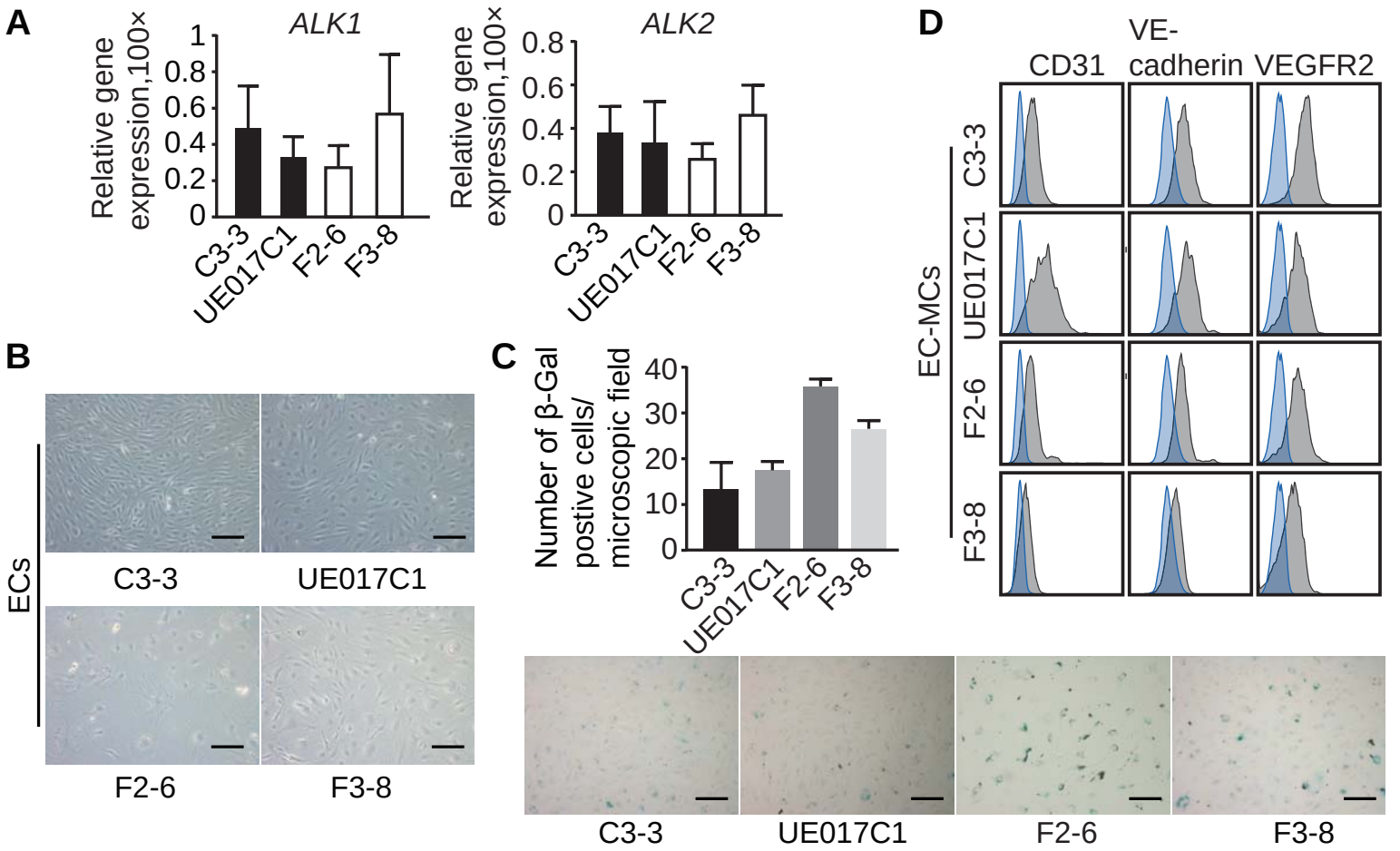
A
ALK1
Relative gene expression,100×
1
0.8
0.6
0.4
0.2
0
C3-3
UE017C1
F2-6
F3-8
ALK2
Relative gene expression,100×
0.8
0.6
0.4
0.2
0
C3-3
UE017C1
F2-6
F3-8
D
CD31
VE-cadherin
VEGFR2
EC-MCs
C3-3
UE017C1
F2-6
F3-8
B
ECs
C3-3
UE017C1
F2-6
F3-8
C
Number of β-Gal postive cells/ microscopic field
40
30
20
10
0
C3-3
UE017C1
F2-6
F3-8
C3-3
UE017C1
F2-6
F3-8

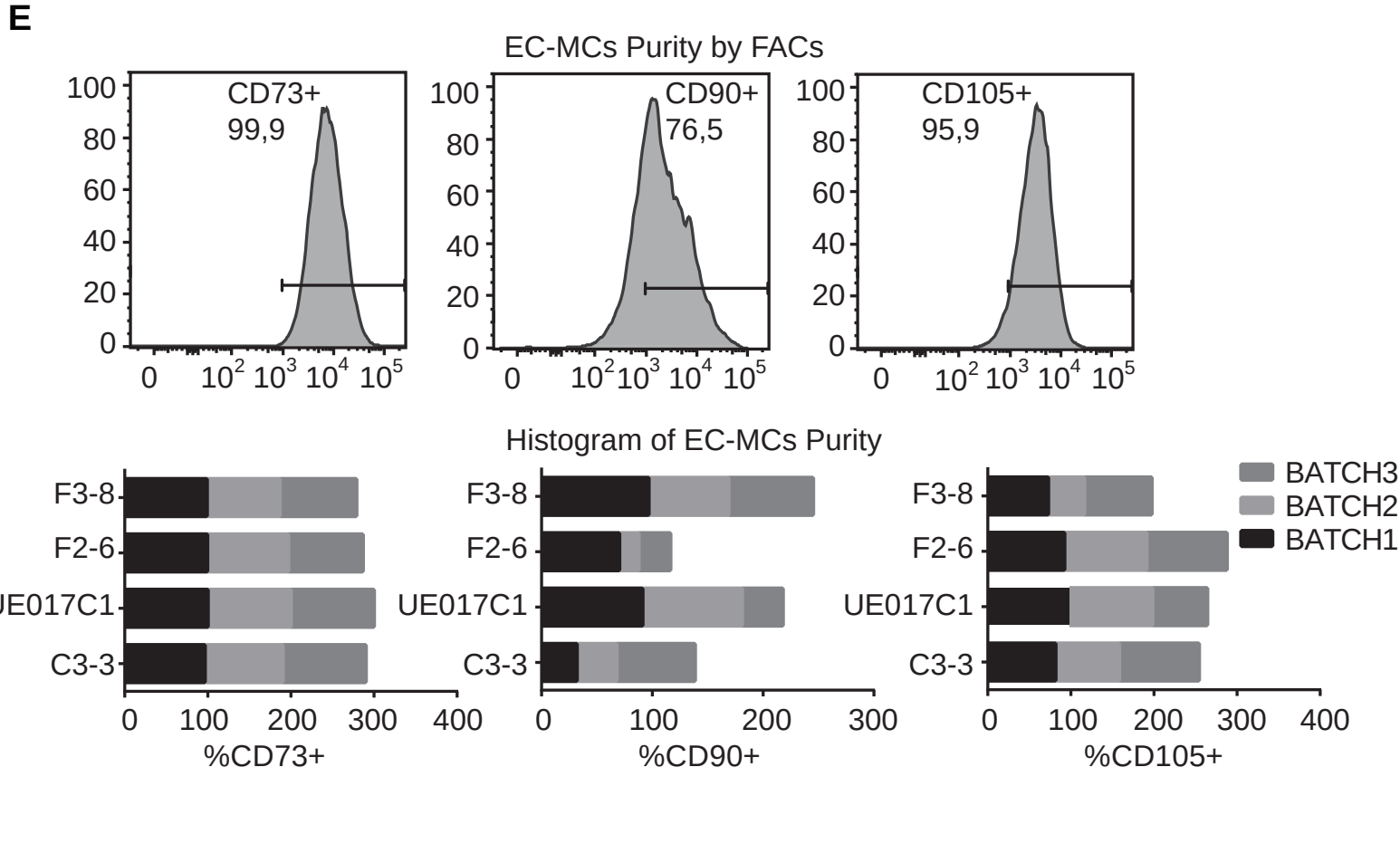
E
EC-MCs Purity by FACs
CD73+
99,9
CD90+
76,5
CD105+
95,9
100
80
60
40
20
0
0
10^2
10^3
10^4
10^5
Histogram of EC-MCs Purity
F3-8
F2-6
UE017C1
C3-3
0
100
200
300
400
%CD73+
%CD90+
%CD105+
BATCH3
BATCH2
BATCH1

Figure S3

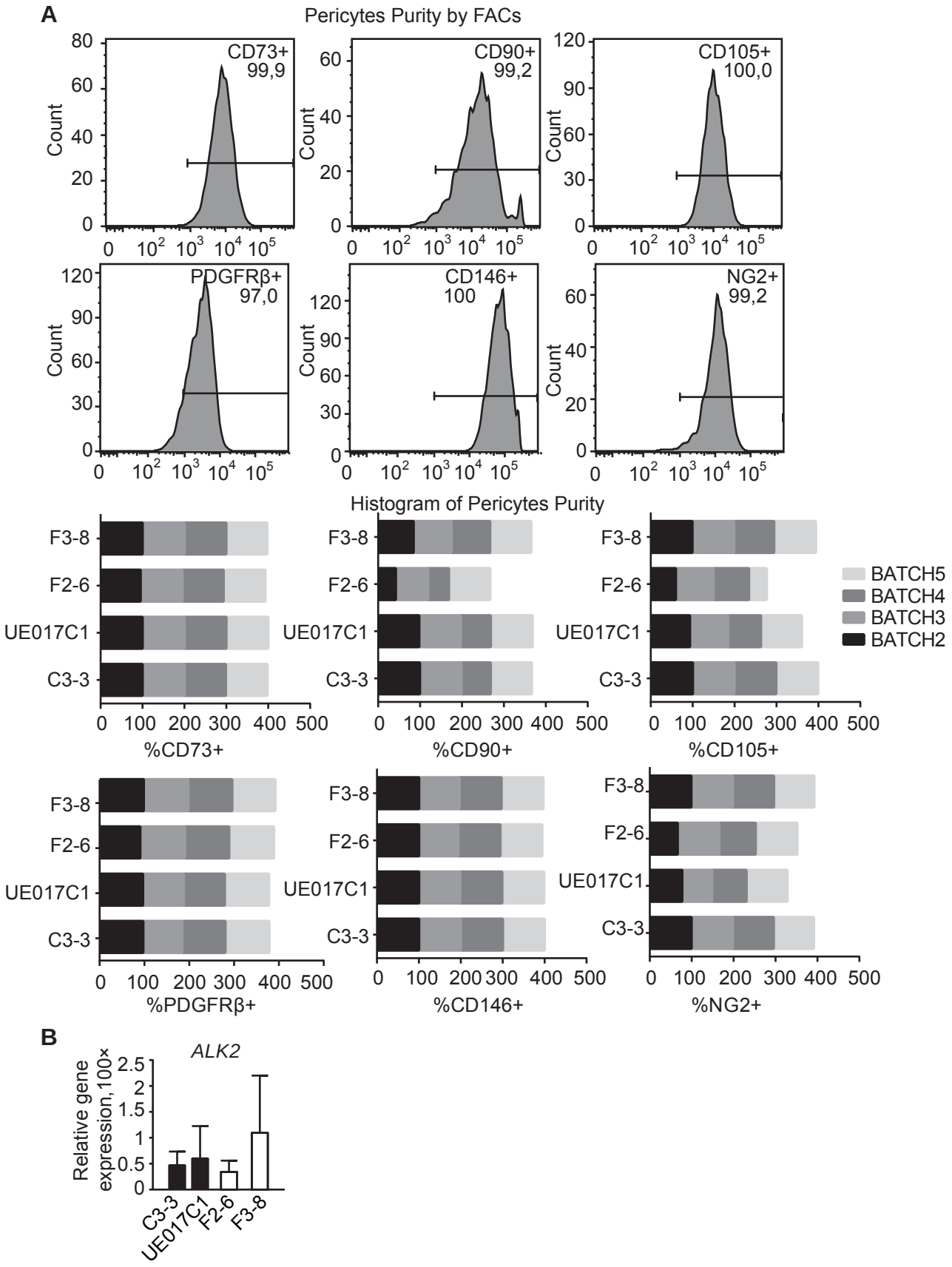
A
Pericytes Purity by FACs
CD73+ 99,9
CD90+ 99,2
CD105+ 100,0
PDGFRβ+ 97,0
CD146+ 100
NG2+ 99,2
Count
Histogram of Pericytes Purity
F3-8
F2-6
UE017C1
C3-3
BATCH5
BATCH4
BATCH3
BATCH2
%CD73+
%CD90+
%CD105+
%PDGFRβ+
%CD146+
%NG2+
B
ALK2
Relative gene expression, 100×
C3-3
UE017C1
F2-6
F3-8

Figure S1. Characterization of hiPSCs from FOP Patients and Healthy Donor

(A) Schematic representation of the reprogramming of hiPSCs from urine cells.

(B) Left panel, bright field image of cultured patient F2 urine cells. Middle panel, bright field image of cultured human FOP hiPSCs. Right panel: ALP staining of FOP hiPSCs. Scale bars, 250 μm.

(C) Sequencing results of the G→A mutation site in the FOP hiPSCs.

(D) Normal karyotypes of FOP hiPSCs and control hiPSCs.

(E) Lack of vector DNA in expanded hiPSCs that have been passaged for >10 times. PCR analysis on total DNA extracted from control and FOP hiPSCs was performed by using primers that specifically recognize exogenous transgenes (exo genes, OCT4, SOX2, KLF4, SV40L, oriP and EBNA1). Endogenous OCT4 (endoOCT4) is used for the detection of OCT4 expression and GAPDH was used as the loading control. Positive control, genome DNA extracted from urine cells that were transfected with related episome vectors. Negative control, water.

(F) qPCR analysis of endogenous *OCT4*, *SOX2*, *NANOG*, and *REX1* mRNA expression in FOP hiPSCs and H1 ESCs. H1 ESCs were used as positive control. *ACTIN* was used to normalize gene expression. Each value is the means ± SD. All the values were adjusted to urine cells value, which is defined as 1. The values represent the average level of 3 independent samples.

(G) Immunofluorescence staining of hiPSCs specific cell markers. Green: antibody indicated in the figure; blue: DAPI. Scale bars, 50 μm.

(H) Hematoxylin/eosin staining of teratoma derived from FOP hiPSCs (F2-6). Scale bars, 100 μm.

(I) Western blot in FOP and control hiPSCs. After serum starvation for 6 hours, hiPSCs were stimulated with or without BMP6 (5ng/ml) for 1 hour. Protein was isolated and western

blotting was performed to check the SMAD1/5 phosphorylation. GAPDH was used as loading control; all the experiments represented 2 independent biological replicates.

Figure S2: hiPSCs-ECs and EC-MCs Characterization. Related to Figure 2.

(A) The mRNA expression level of *ALK1* and *ALK2* in $CD31^+$ ECs. Each value is the means ± SD. All the experiments represented 3 independent biological replicates and were normalized to *ACTIN*.

(B) Bright field image of ECs on passage 3 after cell sorting. Scale bars, 100 μm.

(C) Upper panel: Numbers of β-galactosidase positive cells per microscopic field. Lower panel: Bright field image of β-galactosidase staining of ECs. Scale bars, 100 μm. All the experiments were repeated 3 times, and one of the representative results is shown. Values are presented as mean and SD from 3 technique replicates.

(D) FACs analysis for ECs markers in EC-MCs. Blue, unstained cells; grey, antibody as indicated.

(E) Upper panel: FACs gates illustrating percentage of CD73, CD90 and CD105 positive cells. Lower panel: Histogram of CD73, CD90 and CD105 positive cells analyzed in this study from 3 batches of experiments, the average data from 3 batches of experiments showed in Figure 2F.

Figure S3: hiPSC-pericytes Characterization. Related to Figure 3.

(A) Upper part: FACs gates illustrating percentage of CD73, CD90, CD105, PDGFRβ, CD146 and NG2 positive cells. Lower part: Histogram of CD73, CD90, CD105, PDGFRβ, CD146 and NG2 positive cells analyzed in this study from 4 batches of experiments, the average data from 4 batches of experiments showed in Figure 3A.

(B) The mRNA expression level of *ALK2* in $CD31^-$ pericytes. Each value is the means ± SD. All the experiments represented 3 independent biological replicates and were normalized to *ACTIN*.

Supplemental Experimental Procedures

Ethical Statement

The participants in this manuscript have signed written informed consent for donating human urine cells for stem cell generation. Experiments involved with human subjects was approved by IRB GIBH-IRB02-2009002 at Guangzhou Institutes of Biomedicine and Health (GIBH), and 12/467 (2013 January) at VU university medical center. The animal research was approved by IRB at GIBH (NO. 2010012).

Urine Cell Culture and hiPSCs Generation

Urine cells were collected and maintained as previously publication (Zhou et al., 2011). Urine cells within 5 passages were used for iPS cells generation. hiPSC lines were generated from 5×10^5–1×10^6 urine cells which was electroporated with episomal vectors (3.5 μg pEP4EO2SET2K (contains *OCT4*, *SOX2*, *SV40LT* and *KLF4*) and pCEP4-miR-302-367 cluster (contains *miR-302b, c, a, d* and *miR-367*) by Amaxa™ Basic Nucleofector™ kit for primary mammalian epithelial cells, program T-020 (LONZA). The transfected urine cells were immediately seeded onto matrigel (BD Biosciences, 354230) pre-coated 6-well plates. Refreshed the medium with defined medium mTeSR1 (StemCell Technologies, 05852) with TGFβ/Activin/Nodal receptor inhibitor A-83-01 (Sigma, SML0788), MEK inhibitor PD0325901, GSK3b inhibitor CHIR99021 and ROCK inhibitor thiazovivin (gifts from Dr. Ke Ding) the next day and changed medium every other day. The appeared hiPSCs were passaged by mechanical picking and replated in matrigel pre-coated plates between day 20 and day 30 after induction. The hiPSCs were routinely maintained in mTesR1 medium and passaged by dispase (1 mg/ml in DMEM/F12, Gibco, 17105-041) or by 0.5 mM EDTA (Invitrogen, AM9260G). H1 human embryonic stem cells brought from WiCell Research Institute (Madison, WI). UE017C1 (uiPSC-015 C1 in the paper) was obtained from the Guangzhou Stem Cell Bank and was previously characterized (Xue et al., 2013).

hiPSCs Characterization

qPCR, transgene integration, immunofluorescence (OCT-3/4 Antibody, Santa Cruz Biotechnology sc-5279; Human NANOG Affinity Purified Polyclonal Ab, R&D AF1997; Anti-SSEA4 antibody, Abcam AB16287; Anti-TRA-1-60, Millipore MAB 4360; Anti-TRA-1-81, Millipore MAB 4381) and karyotyping were done as described (Xue et al., 2013); the primers used for transgene integration and qPCR also published before (Xue et al., 2013). For teratomas, hiPSCs were resuspended with 30% matrigel and then injected subcutaneously and intramuscularly into the flanks of SCID mice. Tumors were sectioned after 7 weeks and stained with hematoxylin/eosin.

ALK2 Mutational Analysis

Genomic DNA of hiPSCs was isolated by using Wizard® Genomic DNA Purification Kit (Promega, A1120), PCR reaction was conducted as previous publication using primers as following (Kaplan et al., 2008): Forward primer: 5'-CCAGTCCTTCTTCCTTCTTCC-3', Reverse primer: 5'-AGCAGATTTTCCAAGTTCCATC-3'. PCR products were sequenced to identify the mutation sites.

Differentiation hiPSCs into ECs and Pericytes

ECs and pericytes differentiation was initiated by culture hiPSCs in basal medium BEPL and growth factors Activin A (25ng/ml, R&D, 338-AC-010), BMP4 (30ng/ml, R&D, 314-BP-010/CF), VEGF (30ng/ml, R&D Systems, 293-VE) and the small molecule inhibitor CHIR99021 (1.5μM, Tocris, 4423) for 3 days. The medium was refreshed with BPEL with VEGF and SB43152 (10μM, Tocris, 1614) from day 4 to day 10 of differentiation. ECs were isolated by $CD31^-$ labeled Dynabeads (Life Technologies, 11155D). Sorted $CD31^+$ ECs were maintained in human endothelial growth (serum free) medium (hEC-SFM) (Life Technologies, 11111) supplemented with 1% platelet poor plasma (BTI, BT-214), 30ng/ml VEGF and basic fibroblast growth factor (bFGF) (20ng/ml, R&D, 100-18B) on 0.1% gelatin

(Sigma-Aldrich, G1890) coated plates, and passaged every 3-4 days by TrypLE Select (Gibco, 12563-011). $CD31^-$ cells were plated in EGM-2 media (Lonza, CC-3162). Medium changed to DMEM+10% FBS (Gibco, 10270), supplemented with or without TGFβ3 (1ng/ml, a generous gift of Kenneth K. Iwata, OSI Pharmaceuticals) and PDGF-BB (4ng/ml, Peprotech, 100-14B) for 1 day when cells were confluent. Afterwards, the hiPSCs derived pericytes were routinely maintained in DMEM+10% FBS on gelatin pre-coated plates.

Flow Cytometry (FACs) Analysis

Cells were dissociated by TrypLE Select and washed with the FACs buffer with 10% FBS, followed the other time of washing by the FACs buffer. The following antibodies was used for the FACs staining: VE-cadherin-A488 (eBiosciences, 53-1449-41, 1:100), CD31-APC (eBiosciences, 17-0319, 1:200), KDR-PE (R&D Systems, FAB357P, 1:50), PDGFRβ-PE (BD Pharmingen, 558821, 1:50), CD73-PE (BD Pharmingen, 550257, 1:50), CD105-PE (Life Technologies, MHCD10504, 1:200), CD90-PE (1:400), NG2-PE (R&D, FAB2585P, 1:50), CD146-FITC (BD, P1H12, 1:50). Samples were analyzed with the MACSQuant VYB (Miltenyi) with the following instrument settings Blue/488 FITC, A488: 525/50, Yellow/561 PE: 586/15, APC: 661/20. Unstained cells were used as negative controls for FACS gating. FACS data were analyzed using FlowJo 10.1 software.

Cell senescence assay

β-galactosidase (β-gal) activity was performed using a senescence detection kit (Cell Signaling, 9860S) according to the manufacturer's instructions. The number of β-gal positive cells was counted in randomly selected microscopic fields (magnification ×10).

Alkaline Phosphatase (ALP) Assay

Pericytes were seeded in 96 well plate pre-coated with 0.1% gelatin. After pretreating LDN-212854 (gift from Paul Yu) for 1 day, differentiation of pericytes was initiated in osteogenic medium, which is comprised of α-MEM (Gibco, 32561-029) supplemented with 10% FBS,

0.2 mM ascorbic acid (Sigma, A8960), dexamethasone (Sigma, D4902) and 10 mM of β-glycerophosphate (Sigma, G6251), medium refreshed every 3-4 days. Histochemical examination of ALP activity was performed using naphtol AS-MX phosphate (Sigma, N4875) and fast blue RR salt (Sigma, F0500), as described previously (Shi et al., 2013).

Chondrogenic Differentiation

Chondrocytes differentiation was performed according to previous publication (Greco et al., 2011). Briefly, hiPSC-pericytes were suspended in growth medium at a density of 1.5×10^7/ml, micromasses were seeded in 48-well plates by pipetting 10 µl of cell suspension into each wells. The droplets were leave in the incubator for 3 hours for attachment, after that the growth medium was added. The growth medium was changed to chondrogenic medium (Dulbecco's modified Eagle's medium/F-12 (Invitrogen), 1% (v/v) ITS+ Premix (Corning), 50 µg/ml ascorbic acid, 40 µg/ml L-Proline (Sigma), 0.1 mM dexamethasone, 100 µg/ml sodium pyruvate) 24 hours later and culture for another 3 days before stained with 1% (w/v) Alcian Blue (pH 1.0, Sigma). The quantification of Alcian blue staining was performed by incubated stained micromass with 125 µl 6 M guanidine hydrochloride overnight. The absorbance of the Alcian blue solution was measured at 595 nm to determine the relative amount of bound GAGs in the micromass.

Mineralization assay

The mineralization assay was performed after subsequent 3 weeks of culturing in osteogenic medium. To visualize mineralization, cells were stained with 2% alizarin red S solution (Sigma, A5533).

Western Blotting

Cell lysate was isolated from subconfluent cells cultured for 24 hours in α-MEM+1% FBS. Western blotting was performed as previously described using standard techniques (Shi et al., 2013). The antibodies used for immunoblotting were phosphorylated SMAD1/5 antibody

(1:1000, Cell signaling Technology, Danvers, MA, USA, 9511), SMAD1/5 antibody (1:1000, Santa Cruz, SC-6031) and GAPDH antibody (1:40,000, Sigma). Protein expression was quantification of by ImageJ software (NIH). GAPDH was used as the loading control.

Statistical Analyses

Error bars indicated standard deviation of the mean. We treated each cell line as an individual biological replicate and pooled our results into control group (C3-3 and UE017C1) or FOP group (F2-6 and F3-8). At least three replicates of each of the two control or two FOP hiPSCs or derived cells were performed. Differences between the control group and the FOP group were evaluated by t-test or one-way ANOVA with Tukey's multiple comparison tests by using the Prism Software (6.01 version; GraphPad Software). Differences were considered significance when $p < 0.05$.

qPCR primers used in this study

Markers	Forward primer (5'-3')	Reverse primer (5'-3')
ID1	CTGCTCTACGACATGAACGG	GAAGGTCCCTGATGTAGTCGAT
ID3	CACCTCCAGAACGCAGGTGCTG	AGGGCGAAGTTGGGGCCCAT
ALP	GACCCTTGACCCCCACAAT	GCTCGTACTGCATGTCCCCT
COL1α	CAGCCGCTTCACCTACAGC	TTTGTATTCAATCACTGTCTTGCC
OSC	GAAGCCCAGCGGTGCA	CACTACCTCGCTGCCCTCC
ALK1	ATGACCTCCCGCAACTCGA	TAGAGGGAGCCGTGCTCGT
ALK2	TGCCTTCGAATAGTGCTGTC	CATCAAGCTGATTGGTGCTC
OCT4	ACGACCATCTGCCGCTTTG	GCTTCCTCCACCCACTTCTG
NANOG	GCCGAAGAATAGCAATGGTG	TGGTGGTAGGAAGAGTAGAGG
T	ATCACCAGCCACTGCTTC	GGGTTCCTCCATCATCTCTT
PDGFRα	ATTGCGGAATAACATCGGAG	GCTCAGCCCTGTGAGAAGAC
ETV2	CAGCTCTCACCGTTTGCTC	AGGAACTGCCACAGCTGAAT
CD31	GCATCGTGGTCAACATAACAGAA	GATGGAGCAGGACAGGTTCAG
CD105	CCCGCACCGATCCAGACCACTCCT	TGTCACCCCTGTCCTCTGCCTCAC
PDGFRβ	ACGGAGAGTGTGAATGACCA	GATGCAGCTCAGCAAATTGT
NG2	CCAGGAAAGGCAACCTTCAAC	ACGGAAACGGAAGGTGTCC
ACTIN	AATGTCGCGGAGGACTTTGATTGC	AGGATGGCAAGGGACTTCCTGTAA

PCR Transgene primers

Markers		(5'-3')
OCT4	Oct4-SF1	AGTGAGAGGCAACCTGGAGA
	IRES2-SR	AGGAACTGCTTCCTTCACGA
SOX2	Sox2-SF1	ACCAGCTCGCAGACCTACAT
	SV40pA-R	CCCCCTGAACCTGAAACATA
KLF4	Klf4-SF1	CCCACACAGGTGAGAAACCT
	SV40pA-R	CCCCCTGAACCTGAAACATA
SV40L	SV40T-SF1	TGGGGAGAAGAACATGGAAG
	IRES2-SR	AGGAACTGCTTCCTTCACGA
oriP	pEP4-SF1	TTCCACGAGGGTAGTGAACC
	pEP4-SR1	TCGGGGGTGTTAGAGACAAC
EBNA1	pEP4-SF2	ATCGTCAAAGCTGCACACAG
	pEP4-SR2	CCCAGGAGTCCCAGTAGTCA
endoOCT4	endoOct4-F2	AGTTTGTGCCAGGGTTTTTG
	endoOct4-R2	ACTTCACCTTCCCTCCAACC
GAPDH	GAPDH-F	GTGGACCTGACCTGCCGTCT
	GAPDH-R	GGAGGAGTGGGTGTCGCTGT

Supplemental References

Greco, K.V., Iqbal, A.J., Rattazzi, L., Nalesso, G., Moradi-Bidhendi, N., Moore, A.R., Goldring, M.B., Dell'Accio, F., and Perretti, M. (2011). High density micromass cultures of a human chondrocyte cell line: a reliable assay system to reveal the modulatory functions of pharmacological agents. Biochemical pharmacology *82*, 1919-1929.

Kaplan, F.S., Xu, M., Glaser, D.L., Collins, F., Connor, M., Kitterman, J., Sillence, D., Zackai, E., Ravitsky, V., Zasloff, M., *et al.* (2008). Early diagnosis of fibrodysplasia ossificans progressiva. Pediatrics *121*, e1295-1300.

Shi, S., Cai, J., de Gorter, D.J., Sanchez-Duffhues, G., Kemaladewi, D.U., Hoogaars, W.M., Aartsma-Rus, A., t Hoen, P.A., and ten Dijke, P. (2013). Antisense-oligonucleotide mediated exon skipping in activin-receptor-like kinase 2: inhibiting the receptor that is overactive in fibrodysplasia ossificans progressiva. PloS one *8*, e69096.

Zhou, T., Benda, C., Duzinger, S., Huang, Y., Li, X., Li, Y., Guo, X., Cao, G., Chen, S., Hao, L., *et al.* (2011). Generation of induced pluripotent stem cells from urine. Journal of the American Society of Nephrology : JASN *22*, 1221-1228.